Computers and Mathematics with Applications 64 (2012) 1473–1483

Contents lists available at SciVerse ScienceDirect

Computers and Mathematics with Applications

journal homepage: www.elsevier.com/locate/camwa

Myoelectric activity detection during a Sit-to-Stand movement using threshold methods

Ghulam Rasool [a,*], Kamran Iqbal [a], Gannon A. White [b]

[a] Systems Engineering Department, University of Arkansas at Little Rock, 72204 Little Rock, AR, USA

[b] Health Sciences Department, University of Arkansas at Little Rock, 72204 Little Rock, AR, USA

ARTICLE INFO

Keywords:
Myoelectric signal
Double threshold
Energy detector
Sit-to-Stand movement

ABSTRACT

Myoelectric signals recorded via surface electrodes contain rich muscle activity information that is beneficial for both clinical diagnosis and biomedical research. When synchronized with the kinematic data, these signals provide investigators an insight into muscle activation sequence, onset, levels, and periods. A primary difficulty with the analysis and interpretation of electromyography (EMG) signals lies in the inherent stochastic nature of the EMG process, which arises from its biological variability as well as noise added during the collection process. Various techniques for muscle onset and activity detection from the myoelectric signal have been proposed in the literature. Our focus in this study is myoelectric activity detection from EMG signals collected during Sit-to-Stand (STS) and Stand-to-Sit (STST) movements. We explore a previously established double threshold detection method, and compare its results with a novel detection scheme based on the energy of the signal. Accordingly, EMG signals from four lower extremity muscles, and synchronized kinematic data, were collected for 180 trials of STS and STST movements performed in the laboratory. Detection thresholds above baseline in the case of both algorithms were computed and analyzed using a 2 (detectors) $\times$ 4 (activity thresholds) repeated measures analysis of variance. Our statistical analysis revealed that the energy detection method performed similarly to the double threshold method, while both methods required a considerably higher threshold above baseline for detection.

1. Introduction

The STS and STST transfers are functional movements routinely performed by a majority of the population. Though simple in appearance, the underlying coordination of the musculoskeletal dynamics necessary to ensure successful STS and STST transitions are quite complicated. Clinical studies attempting to diagnose deficiencies in daily functional movements stand to benefit from precisely identifying muscle onset/offset and periods of muscle activation during different phases of the movement. Detection of muscle activity from EMG signals in STS and STST movements will benefit daily functional movement analysis of patients with clinical conditions such as stroke [1,2] and Parkinson's disease [3,4] as these applications require an accurate detection of onset, offset, and duration of the EMG burst.

Voluntary muscular activity results in an EMG signal that increases in magnitude due to increment in the number of recruited motor units and/or increased frequency of the motor unit (MU) firing rates. Generally, application areas of surface EMG signal include: [5] (1) the activation timing of muscles, (2) the force/EMG signal relationship, and (3) the use of the EMG signal as a fatigue index. In this paper, we focus on the first application area i.e., the timing and duration of muscle

* Corresponding author. Tel.: +1 501 319 2167.
E-mail address: gxrasool@ualr.edu (G. Rasool).

0898-1221/$ – see front matter © 2012 Elsevier Ltd. All rights reserved.
doi:10.1016/j.camwa.2012.03.094

activation and explore a new method in an attempt to accurately determine muscle activity periods during STS and STST transfers.

Several methods are described in the literature for detecting the onset and duration of muscle activation. These range from simple heuristic algorithms to optimal statistical techniques and wavelets based algorithms. For example, Di Fabio used a 50 sample window of the EMG signal to make a baseline reference, consequently the muscle was considered ON if 25 consecutive samples exceeded three standard deviations (σ) of the mean baseline activity [6]. The EMG signal was full-wave rectified and low pass filtered before application of the detection algorithm. Lidierth proposed a detection method which was identical to Di Fabio with extended post-processing procedures in an to improve detection results [7]. Hodges and Bui also used the same algorithm as Di Fabio, yet compared different window sizes, low pass filter frequencies and one, two or three standard deviations (σ) above base line to examine differences in threshold selections [8]. The authors used EMG signals that were rectified before application of the detection algorithm. Results were then compared to human experts to see the effects of different parameters. Abbink et al. proposed a method based on Hodges and Bui with a change of cut-off frequency and window length to optimize detection of muscle activation periods [9]. Algorithms used by [6–9] can be classified as more of a heuristic approach based upon defining a baseline and then detecting muscle activity using various thresholds.

Bonato et al. provided another perspective to muscle activity detection schemes which was a statistical method based upon two thresholds, called the double threshold method and presented Receiver Operator Characteristic (ROC) curves for performance of double threshold method [10]. EMG signals were whitened (de-correlated) before application of their detection algorithm, but methods of de-correlating EMG signal were not discussed. Generalized Likelihood Ratio (GLR) test was proposed by Micera et al. to find muscle activity onset from the EMG signal [11]. Staude extended the statistical methods to include other optimal change detection algorithms based on cumulative sum type (CUSUM) and Approximated Generalized Likelihood Ratio (AGLR) [12]. Despite the complexity of the likelihood ratios algorithms proposed by Micera [11] and Staude [12] in their implementation to the EMG signal, Staude states his method is appropriate for real-time applications. Staude et al. later presented an overview of different techniques based upon thresholds and statistical optimal decision methods [13]. Due to non-stationary nature of the EMG signal, wavelet transforms are also used by some authors for the purpose of detecting of muscle activations [14,15], but again these methods suffer from implementation complexity. Solnik et al. used the Teager–Kaiser Operator to improve the detection accuracy but used the algorithms proposed by [10,12,16].

There has been considerable work on finding the mathematical/statistical relation between the movement being performed and the resulting EMG signal. Bobet and Norman [17] used least-squares fitting to find a dynamic relationship between EMG and joint moments for making joint movement predictions. Furthermore, some algorithms have been proposed to find a relationship between EMG signal and the specific movement being performed [18]. Moreover, modeling efforts have been done using fractional derivatives [19]. A majority of the literature examining these methods of muscle activity detection apply these to human gait. Whether these methods of determining muscle activation during gait will similarly work for the STS and STST movements has not been investigated.

In this study we aim to detect muscle activation periods in the myoelectric signals recorded from multiple sites during STS and STST movements. We use a previously established double threshold [10] detection scheme, and we propose another scheme based upon the Neyman–Pearson detector formulation for stochastic signals buried in noise, called the energy detectors. A exhaustive literature review did not reveal any previous studies which applied the energy detectors to myoelectric signals. We compare ROC curves of both detection schemes to determine which of them more precisely identifies the onset and duration of muscle activation.

2. Methods

The study received prior approval from Institutional Review Board (IRB) of University of Arkansas at Little Rock (UALR) under protocol 12-054 and all participants provided written informed consent. Eighteen healthy individuals, three males and fifteen females, volunteered for the study. The participants mean ($\pm$ S.D.) age, height, and body mass were 21.94 $\pm$ 5.05 years, 1.70 $\pm$ 0.04 m, and 66.76 $\pm$ 4.32 kg respectively. All participants were free from current or pre-existing injuries that would influence their execution of the STS or STST movements.

2.1. Protocol

Numerous factors give rise to variability in the performance of the STS and STST movements [20]. These factors can be termed as determinants of the STS and STST transfers. Relevant determinants which were controlled during this study are:

1. Each individual's seat height was set equal to his/hers knee height as measured from the lateral epicondyle of the femur to the floor without shoes. All trials were performed barefoot.
2. The seat used in this study, which was a common adjustable height chair, did not have a backrest or armrests. The chair was placed comfortably in front of dual force plates for measuring the ground reaction forces (GRF) under each foot, which were recorded but not presented here.

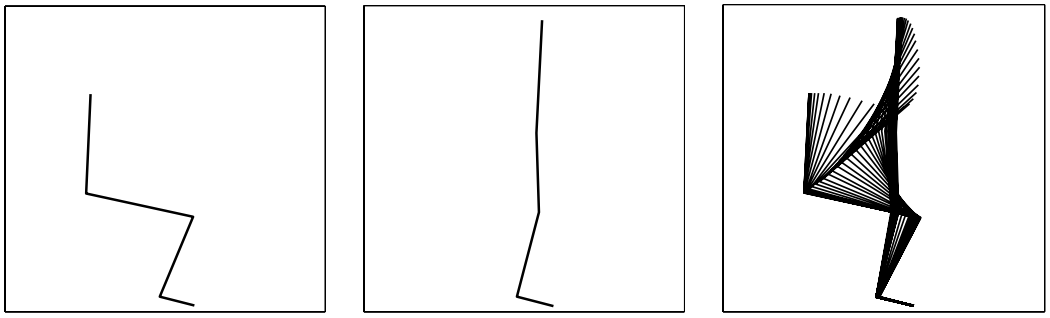

(a) Sitting position. (b) Standing position. (c) Complete movement.

Fig. 1. Positions for STS and STST movements: (a) Sitting position, which is the initial position for the STS movement and terminating position for the STST movement; (b) Standing position, which is the terminating position for the STS movement and initial position for the STST movement; (c) Movement profile during the STS movement showing all five markers joined by stick figures.

3. Participants were instructed to position their arms/hands in the most natural manner that did not place them near any EMG electrodes so as not to interfere with the data collection. Furthermore, participants were instructed to perform the STS and STST movements without utilizing their arms/hands to push-off their legs or chair.
4. Participants were asked to stand, and sit a total of 15 times in groups of five. After participants visually appeared to stabilize during the standing portion of each trial, which took 3–5 s, they were asked to sit. Between each group of five STS–STST trials, participants were asked to take a short break by walking around the room briefly.

2.2. Kinematic data recording

Spherical reflective markers were fixed to the fifth metatarsal (toe), lateral malleolus (ankle joint), lateral epicondyle of the femur (knee joint), lateral aspect of the greater trochanter (hip joint) and the lateral aspect of the acromion of the scapula using a double-sided adhesive tape. The anatomical landmarks were selected to allow for calculation of sagittal plane kinematics using a four segment rigid-link model of the body. Marker data was recorded at 100 Hz using the Vicon Nexus 1.7.1 (Vicon Motion Systems CA 90066, USA) and ten Bonita family series cameras. Sitting and standing positions for subjects are shown in Fig. 1(a) and (b). Transition from sitting to standing position discretized at certain intervals is shown in the Fig. 1(c). Raw marker data (position coordinates of markers with reference to laboratory/world frame) was exported to and processed using MATLAB (version 7.1.2. Natick, Massachusetts: The MathWorks Inc.). Segmental angles for the torso, thigh and shank were calculated with respect to horizontal axes extending from the hip, knee and ankle markers respectively. All angles are measured positive counter-clockwise.

2.3. EMG data recording

A Noraxon TeleMyo DTS Wireless EMG system was used to record EMG data via the Vicon Nexus system at sampling rate of 1500 Hz. Electrodes (dual electrodes with a 2 cm inter-electrode distance) were placed on each participant's right side over the muscle bellies of the soleus, tibialis anterior, biceps femoris and rectus femoris. The right side is commonly chosen to minimize recording of the ECG signal. Skin preparation, and all related precautions for recording of EMG data were taken. The EMG signal delay specified by the recording device (312 ms at 1500 Hz) was compensated for within in the Vicon Nexus software.

3. EMG signal and its pre-whitening

3.1. Adaptive pre-whitening filter

In both detection schemes presented in this paper, besides the assumption of the recorded EMG signal being Gaussian, it has been assumed that samples are also uncorrelated. This assumption is not true and there is a need to de-correlate/whiten it before applying both detection algorithms. A pre-whitening filter based on Staude [12] is proposed here, but an essential element of this filter i.e., its order (p), is missing in the original scheme, and for which we propose the Ljung–Box Q-test [21]. Pre-whitening of the EMG signal is achieved based upon estimation of autoregressive (AR) parameters of the observed EMG signal. The EMG signal is modeled as zero-mean discrete white Gaussian noise process $(W_k)_{k\geq 1}$ which excites a linear system with transfer function $H(z)$. Here $(W_k)_{k\geq 1}$ represents discharge timing and recruitment of elementary signal sources

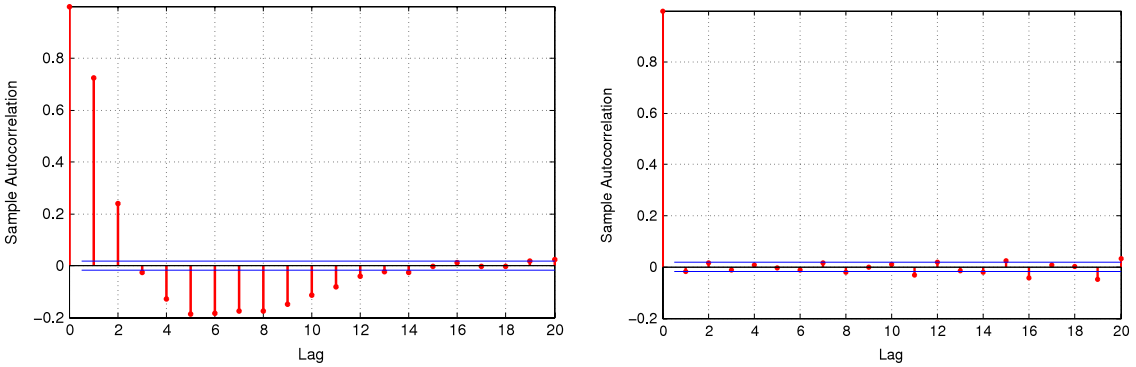

(a) Before pre-whitening filter.

(b) After pre-whitening filter.

Fig. 2. Autocorrelation sequence for the residuals (of the EMG signal fitted to the AR model) before and after pre-whitening filter selected through the Ljung–Box Q-test.

involved, and $H(z)$ represents shape of action potentials and biological transfer function between $(W_k)_{k\geq 1}$ generator and recording site of the EMG signal (i.e. the human skin). It has been proposed to model $H(z)$ as an all pole AR filter of order (p).

$$H(z) = \frac{1}{1 + a_1 z^{-1} + a_2 z^{-2} + \cdots + a_p z^{-p}}, \tag{1}$$

where, $a_i s,\ i = 1, \ldots, p$ are the AR coefficients and z represents the Z-transform. The change to be detected is assumed to predominantly affect the $(W_k)_{k\geq 1}$, and the properties of $H(z)$ remain approximately constant in this change (before and after muscle contraction which is reflected in EMG signal). Therefore, information in AR parameters (a_i) is not related to the change that we are trying to detect and we may remove the irrelevant component of the signal before application of the detection algorithm. The measured EMG signal is filtered by a MA (moving average) filter with a transfer function $H_w(z)$ given by

$$H_w(z) = 1 + b_1 z^{-1} + b_2 z^{-2} + \cdots + b_p z^{-p}, \tag{2}$$

where, $b_j s,\ j = 1, \ldots, p$ are the MA parameters and will be used as filter coefficients to whiten EMG signal.

3.2. The model order (p) of the pre-whitening filter

In order to use the proposed filter, we must decide about the model order (p), where the samples in EMG signal are uncorrelated. We propose to use the Ljung–Box Q-test for this purpose [21]. This *portmanteau* test assesses the null hypothesis that the series of residuals exhibits no autocorrelation for a fixed number of lags (m) against the hypothesis that the autocorrelation sequence is non-zero. Under the null hypothesis asymptotic distribution of Q-statistic is χ^2 with m degrees of freedom. This test is called *portmanteau* as the null hypothesis is well defined but the alternate hypothesis is more loosely defined. We used a 95% confidence interval in this test. This test is performed for an increasing number of AR model order, and a parsimonious AR model is chosen i.e. null hypothesis is established. Results from the pre-whitening filter after parsimonious selection of the AR model order through Q-test are shown in Fig. 2. The procure for selection of pre-whitening filter for the EMG signal can be summarized as follows;

1. Estimate AR parameters by fitting the EMG signal to the AR model.
2. Perform the Q-test on residuals. In case Q-test rejects the null hypothesis, we increased the filter order, i.e., AR model order by one until we failed to reject the null hypothesis establishing the fact that residuals are uncorrelated.
3. We observed that in most of the EMG signals, we failed to reject the null hypothesis at an AR model order of $p = 30$–40.

4. Muscle activity detection via double threshold detector

The surface EMG signal may be considered as a zero-mean Gaussian process $s(t) \in \mathcal{N}(0, \sigma_s^2)$ modulated by the muscle activity and corrupted by an independent zero-mean Gaussian additive noise $n(t) \in \mathcal{N}(0, \sigma_n^2)$. The sampled values are first filtered by a pre-whitening filter (Section 3.1). Let, $\tilde{x}_i$ represent the output of the pre-whitening filter. In the double threshold detection, squared values of two successive samples of the pre-whitening filter output are summed to obtain an auxiliary time series (z_i).

$$z_i = \tilde{x}_{2i}^2 + \tilde{x}_{2i-1}^2. \tag{3}$$

Due to the underlying hypothesis of Gaussianity of the process $s(t)$ and the noise $n(t)$, the pre-whitening filter guarantees the independence of successive samples, and consequently series z_i has a χ^2 distribution with two degrees of freedom. Due to the critical role played by the variances of the signal $s(t)$ and noise $n(t)$ in the detection process, it is important to derive the probability density of the auxiliary time series as an explicit function of the noise variance ($\sigma_{\tilde{n}}^2$). Probability density function (PDF) of z_i when only noise is present is given as:

$$f(z) = \frac{1}{2\sigma_{\tilde{n}}^2} e^{-z/2\sigma_{\tilde{n}}^2} U(z), \tag{4}$$

where $U(z)$ is unit step function. This equation has been derived using basic definitions, i.e.,

$$F_z(z) = \Pr[Z \leq z] = \Pr[\tilde{x}_{2i}^2 + \tilde{x}_{2i-1}^2 \leq z]. \tag{5}$$

We define P_ζ as the probability that a specific noise sample is above a fixed threshold (ζ, also termed as the first threshold by the authors)

$$P_\zeta = P[z > \zeta, x(t) = n(t)] = \int_\zeta^\infty f(z)dz = e^{-z/2\sigma_{\tilde{n}}^2}. \tag{6}$$

When both signal and noise are present in the observed sample, we write PDF of the χ^2 distribution as:

$$f(z) = \frac{1}{2(\sigma_{\tilde{n}}^2 + \sigma_{\tilde{x}}^2)} e^{-z/2(\sigma_{\tilde{n}}^2 + \sigma_{\tilde{x}}^2)} U(z). \tag{7}$$

With (7), we can define probability P_{dk} when the kth sample is above the threshold, as:

$$\begin{aligned} P_{dk} &= P[z > \zeta, x(t) = n(t) + s(t)] = \int_\zeta^\infty f(z)dz = e^{-z/[2(\sigma_{\tilde{n}}^2 + \sigma_{\tilde{s}}^2)]}, \\ P_{dk} &= e^{-\zeta/[2\sigma_{\tilde{n}}^2(1+10^{\mathrm{SNR}/10})]}. \end{aligned} \tag{8}$$

In (8), the signal to noise ratio (SNR) is defined as:

$$\mathrm{SNR} = 10\log_{10}\left(\frac{\sigma_{\tilde{s}}^2}{\sigma_{\tilde{n}}^2}\right). \tag{9}$$

Thus P_{dk} is related to P_ζ as:

$$P_{dk} = e^{(\ln P_\zeta)/(1+10^{\mathrm{SNR}/10})}. \tag{10}$$

The double threshold technique consists of selecting a first threshold ζ and observing m successive samples: if at least r_o out of m successive samples are above the first threshold ζ, the presence of the signal is acknowledged. In this approach, the second threshold is represented by r_o. This relation is obtained by considering the repeated Bernoulli trials. The probability $P_{r_o}(r \geq r_o; m)$, that at least r_o samples out of m cross the threshold is given by as:

$$P_{r_o}(r \geq r_o; m) = \sum_{k=r_o}^{m} \binom{m}{k} P^k (1-P)^{m-k}. \tag{11}$$

Now, we can write the probability of false alarm (P_{FA}) and probability of detection (P_D). P_{FA} is the probability that noise samples are incorrectly interpreted as signal and can be obtained from (11) by putting $P = P_\zeta$

$$P_{\mathrm{FA}} = \sum_{k=r_o}^{m} \binom{m}{k} P_\zeta^k (1-P_\zeta)^{m-k}. \tag{12}$$

P_D is the probability that signal samples, although corrupted by noise, are correctly recognized, and it is obtained by substituting P with P_{dk} in (11) as:

$$P_D = \sum_{k=r_o}^{m} \binom{m}{k} P_{dk}^k (1-P_{dk})^{m-k}. \tag{13}$$

Essentially, we use the following algorithm for detection of muscle activity from noisy myoelectric signal.

The double threshold algorithm;

1. Select $m = 5$, $r_o = 1$ and $P_{FA} = 0.05$, (at some places, we use $P_{FA} = 0.01$ and we will make exclusive mention of that).
2. Raw EMG signal, x_i, is whitened with a pre-whitening filter to get $\tilde{x}_i$, in which all samples are uncorrelated (within a certain statistical confidence interval).
3. Squared values of two successive samples from series $\tilde{x}_i$ are summed and the auxiliary sequence z_i is generated.
4. Variance of the noise $\sigma_{\tilde{n}}^2$ is estimated during a quite seated portion of the trial keeping in view that no voluntary muscle activation has occurred in the selected time interval.
5. P_ζ is calculated from (12), which will be an mth order polynomial and root lying between 0 and 1 is selected.
6. Using $\sigma_{\tilde{n}}^2$ and P_ζ, the threshold ζ is calculated using (6). Here, we use statistical tables of a χ^2 distribution with 2-degrees of freedom (DOF).
7. Sequence of z_i is compared with ζ to determine if activation of the muscle is occurring.
8. Post-processing is done in the detected signal to remove spurious detections.

After implementation in MATLAB, results comparable to [10] were achieved.

5. Muscle activity detection via the energy detector

An energy detector is based upon the Neyman–Pearson lemma and log-likelihood ratio test [22]. Considering N samples of surface EMG signal $x[n] : n = 0, 1, 2 \ldots N-1$ as a zero-mean Gaussian process $s[n] \in \mathcal{N}(0, \sigma_s^2)$ modulated by the muscle activity and corrupted by an independent zero-mean Gaussian additive noise $w[n] \in \mathcal{N}(0, \sigma_n^2)$. The detection scheme is to distinguish between the hypothesis:

$$\begin{aligned} H_o &: x[n] = w[n], \\ H_1 &: x[n] = s[n] + w[n]. \end{aligned} \tag{14}$$

The Neyman–Pearson detector decides H_1 if the likelihood ratio exceeds a threshold γ:

$$L(\mathbf{x}) = \frac{p(\mathbf{x} : H_1)}{p(\mathbf{x} : H_o)} > \gamma, \tag{15}$$

where $p(\mathbf{x} : H_o)$ and $p(\mathbf{x} : H_1)$ are the PDFs of the recorded EMG signal under hypothesis H_o and H_1 respectively, given as:

$$\begin{aligned} H_o &: x[n] \in N(0, \sigma_n^2), \\ H_1 &: x[n] \in N(0, \sigma_n^2 + \sigma_s^2). \end{aligned} \tag{16}$$

By substitution of these PDFs in (15), we get

$$L(\mathbf{x}) = \frac{\frac{1}{[2\pi(\sigma_s^2+\sigma_n^2)]^{N/2}} \exp\left[-\frac{1}{2(\sigma_s^2+\sigma_n^2)} \sum_{n=0}^{N-1} x^2[n]\right]}{\frac{1}{[2\pi\sigma_n^2]^{N/2}} \exp\left[-\frac{1}{2\sigma_n^2} \sum_{n=0}^{N-1} x^2[n]\right]}. \tag{17}$$

Solving for log-likelihood ratio i.e. $l(\mathbf{x}) = \ln(L(\mathbf{x}))$ and formulating a test static function $T(\mathbf{x})$ of available data $x[n]$ as:

$$T(\mathbf{x}) = \sum_{n=0}^{N-1} x^2[n]. \tag{18}$$

The Neyman–Pearson detector decides H_1 if $T(\mathbf{x}) > \acute{\gamma}$, where $\acute{\gamma}$ is the threshold calculated using a P_{FA} specified by the user. The Neyman–Pearson detector computes energy in the received signal and compares it to a threshold $\acute{\gamma}$ and decides about muscle activity onset when a test statistic $T(\mathbf{x})$ is greater than $\acute{\gamma}$ and is therefore named an energy detector. We can study characteristics of this detector using a χ^2 distribution, by noting that $\mathbf{x}$ consists of N independent and identically distributed (*i.i.d.*) Gaussian random variables. $T(\mathbf{x})$ and variance of $x[n]$ under H_o and H_1 can written for χ_N^2 as:

$$\begin{aligned} H_o &: \frac{T(\mathbf{x})}{\sigma_n^2} \in \chi_N^2, \\ H_1 &: \frac{T(\mathbf{x})}{\sigma_n^2 + \sigma_s^2} \in \chi_N^2. \end{aligned} \tag{19}$$

If, we define the right tail probability of a χ^2_N random variable as [22]:

$$Q_{\chi^2_N}(x) = \int_x^\infty p(t)dt. \tag{20}$$

Then, we can write P_{FA} as:

$$\begin{aligned} P_{\text{FA}} &= \Pr[T(\mathbf{x}) > \acute{\gamma}|H_o] = \Pr\left[\frac{T(\mathbf{x})}{\sigma_n^2} > \frac{\acute{\gamma}}{\sigma_n^2}|H_o\right], \\ &= Q_{\chi^2_N}\left(\frac{\acute{\gamma}}{\sigma_n^2}\right). \end{aligned} \tag{21}$$

Upon availability of estimate of σ_n^2, we can use (21) to calculate value of $\acute{\gamma}$ as given below:

$$\acute{\gamma} = \sigma_n^2 Q^{-1}_{\chi^2_N}(P_{\text{FA}}). \tag{22}$$

Essentially, (22) is used to calculate the value of threshold $\acute{\gamma}$ in this detection scheme, once P_{FA} is fixed by the user. Also, for P_D, we have:

$$\begin{aligned} P_D &= \Pr[T(\mathbf{x}) > \acute{\gamma}|H_1], \\ &= \Pr\left[\frac{T(\mathbf{x})}{(\sigma_n^2+\sigma_s^2)} > \frac{\acute{\gamma}}{(\sigma_n^2+\sigma_s^2)}\middle| H_1\right], \\ &= Q_{\chi^2_N}\left(\frac{\acute{\gamma}}{\sigma_n^2+\sigma_s^2}\right). \end{aligned} \tag{23}$$

Using definition of SNR from (9), we can write P_D in terms of P_{FA} using (22) and (23) as:

$$\begin{aligned} P_D &= Q_{\chi^2_N}\left(\frac{\acute{\gamma}}{(\sigma_n^2+\sigma_s^2)}\right) = Q_{\chi^2_N}\left(\frac{\sigma_n^2 Q^{-1}_{\chi^2_N}(P_{\text{FA}})}{(\sigma_n^2+\sigma_s^2)}\right), \\ &= Q_{\chi^2_N}\left(\frac{Q^{-1}_{\chi^2_N}(P_{\text{FA}})}{1+10^{\text{SNR}/10}}\right). \end{aligned} \tag{24}$$

We can use (24) to plot ROC curves to gain an insight into the performance of the energy detector. Once the SNR is estimated (in case of an actual EMG signal) or fixed (in case of a synthetic signal), we draw these curves for a range of values for P_D plotted as a function of P_{FA}. ROC curves provide an insight into the detection scheme and highlight the limitations i.e., trade-off associated with the detection scheme. It is evident from Fig. 3 that we have limitations on reducing the P_{FA}, i.e., P_D also reduces and which in turn implies that we will have greater probability of a miss (defined as: $P_{\text{miss}} = 1 - P_{\text{FA}}$). Therefore, we cannot reduce P_{FA} arbitrarily.

We summarize the algorithm for the energy detection scheme as:

Energy based detection algorithm

1. The EMG signal is whitened (de-correlated) using a pre-whitening filter.
2. A window of ten (or any number of samples selected by user) successive samples is created to form the test statistic (18).
3. Variance of the noise σ_n^2 is estimated during a quite seated portion of the trial keeping in view that no voluntary muscle activation has occurred in the selected time interval.
4. Using P_{FA} fixed by the user, (22) is used to compute the threshold $\acute{\gamma}$.
5. The test statistic $T(\mathbf{x})$ is compared with a threshold $\acute{\gamma}$ to detect of onset of muscle activity; if $T(\mathbf{x})$ is greater than $\acute{\gamma}$, the starting time of the window is marked as starting time for muscle activity; otherwise the window is advanced by one sample.
6. All samples are scanned in this way and positions of onset of activity are marked.
7. Post-processing, similar to the double threshold method, is done in the detected signal to remove spurious detections.

Fig. 4 provides a comparison of both detection schemes using their ROC curves at two different SNR values, 1 and 6. Number of samples marked for both detectors to make a decision about the onset of muscle activity is 10, i.e., within 10 samples decision of the onset of muscle activity will be done by the detectors. The double threshold detector uses 10 samples

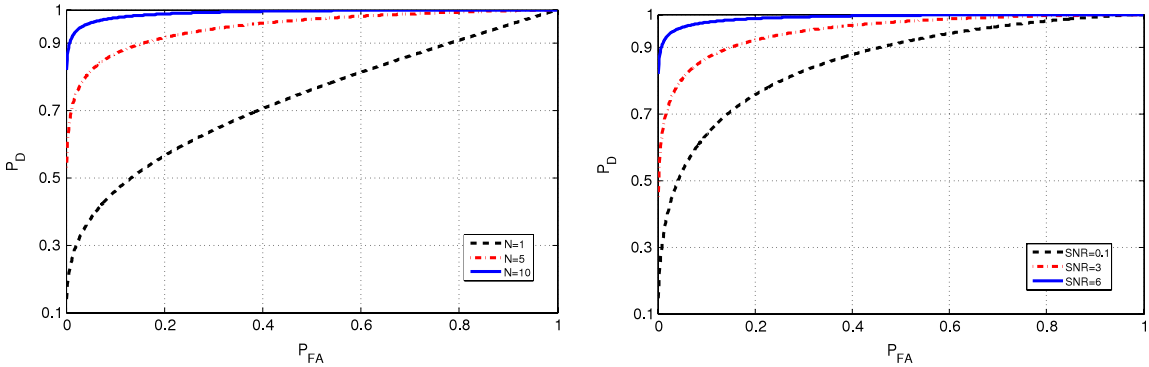

(a) SNR = 6 and $N = 1, 5, 10$. (b) $N = 10$ and SNR = 0.1, 3, 6.

Fig. 3. ROC curves for the energy detector under two different parameters variations: (a) effect of varying window size; and, (b) effect of varying SNR at fixed window size ($N = 10$).

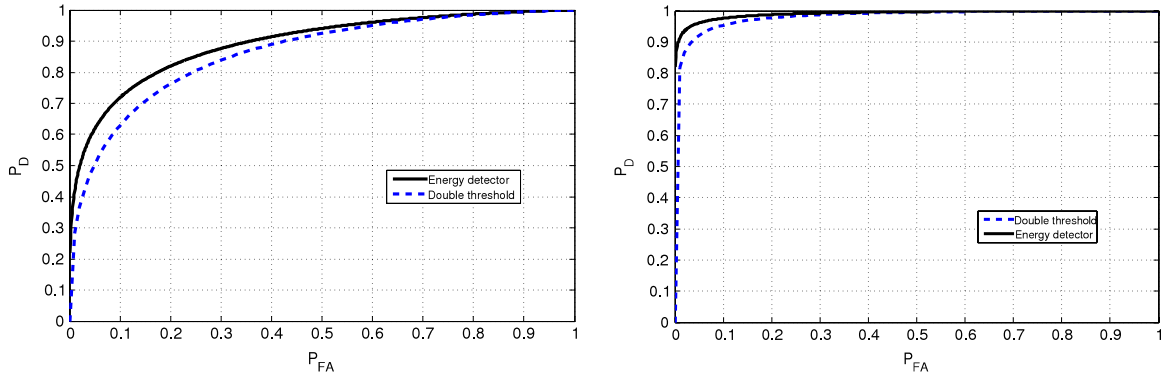

(a) SNR = 1. (b) SNR = 6.

Fig. 4. Comparison of ROC curves for the double threshold and energy detection schemes using ten samples from the EMG signal.

to construct five samples of the auxiliary series, while the energy detector uses them to calculate the test statistic $T(\mathbf{x})$. It is evident from Fig. 4 that energy detector performance is better for both low and high SNR values, i.e., it gives a high probability of detection at a lower probability of false alarm given that both detectors use the same number of samples from a whitened EMG signal.

6. Detection results for STS and STST movements

6.1. Statistical comparison of detection methods

A difficulty faced during the detection process is that during both STS and STST movements, the soleus, bicep femoris and rectus femoris signals continue to be relatively noisy during the standing position. This may be due to their role in helping to maintain postural stability. Therefore, the challenge for detection of muscle activations from these noisy signals is two-fold; the EMG signals are noisy; and the muscles remain active for unspecified periods of time with unknown activation levels. Since, this study sought to explore a novel detection method, it was desirable to analyze signals with minimal noise. Therefore, we chose only to apply the detection methods to the tibialis anterior signals as they had more clearly defined periods of activation.

To make a statistical comparison of the two detection methods, the mean standard deviation (SD) increase above baseline was determined. The mean voltage of the first 500 samples of each trial was computed while each participant sat quietly. This represented the baseline activation level. The SD was also calculated from the first 500 samples. Next, a 45 sample average sliding window was computed for each signal. Finally, the difference between the voltage of a frame identified by a detector and the mean baseline was divided by the SD. This yielded the mean SD increase above baseline and was the value for each trial entered into the statistical analysis. Though collecting/analyzing multiple trials from an individual would typically violate the assumption of independence, [23] details the usefulness/appropriateness of analyzing multiple trials from one individual. Therefore, 270 total trials from 18 individuals were included in the statistical analysis. To control for the probability of committing a type I error, a conservative alpha was chosen ($p < 0.01$) to determine significant differences.

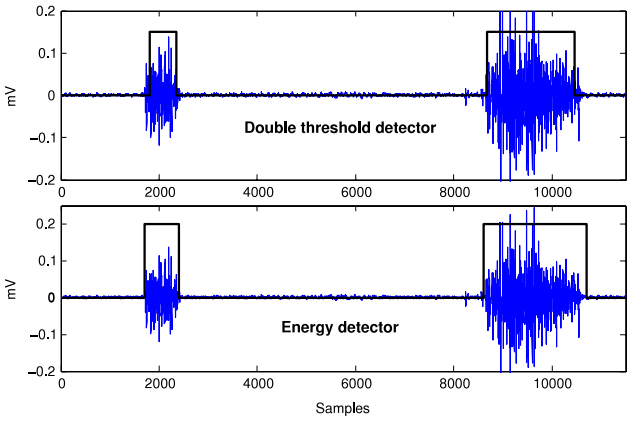

Fig. 5. Detection results from both detectors for the muscle tibialis anterior during STS and STST movement. First envelop represents muscle activity from STS and second, STST movement.

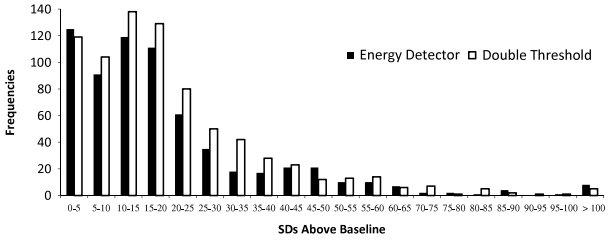

Fig. 6. Detection threshold frequencies.

The primary focus was to examine potential mean threshold differences in the Detector main effect and at what mean SD above baseline they classified muscle activation. The null hypothesis tested was that there would be no differences between the two detectors for any of the activation events. Thresholds were analyzed using a 2×4 repeated measures analysis of variance. The main effect Detector had two levels (Energy Detector and Double Threshold) while the main effect Event had four levels (STS on, STS off, STST on, STST off). Fig. 5 depicts each detector identifying the muscle activation on/off times for the STS and STST transfers. The main effect Detector did not indicate a significant difference between the energy detector and double threshold methods $F(1157) = 1.85, p = 0.176$. The main effect Event did indicate a significant difference $F(3471) = 4.14, p = 0.008$ and post hoc comparisons indicated that the threshold required to determine muscle off for the STS and STST differed ($p < 0.005$). There was no significant interaction $F(3471) = 1.70, p = 0.165$.

The non-significant finding for the main effect Detector indicates the energy detection method performs similarly to the double threshold method. However, both the energy detector (Mean $\pm$ SD $=$ 19.71 $\pm$ 19.71) and the double threshold method failed to classify muscle activation (20.25 $\pm$ 17.91) until much higher SDs above baseline (Fig. 6) than the typical 1, 2, 3 SD threshold [8]. Furthermore, the skewness for each detector was well above normal distribution values (Energydetector $= +2.58$, DoubleThreshold $= +2.07$) indicating each had multiple high detection threshold values. In the future, an optimization analysis should be conducted to determine an optimal range for P_{FA} to detect muscle activation at thresholds above baseline consistent with the literature [24,25].

6.2. Probabilities of detection and false alarm

Muscle activation period detection is the identification of muscle on/off timings with maximum possible accuracy. However, as discussed often in the detection literature, the probability of a false alarm P_{FA} and the probability of detection P_D are directly related. Once P_{FA} is reduced in order to reduce false detections, the probability of detection P_D of muscle activities in the EMG signal also reduces (thereby increasing probability of a miss, P_{miss}). In other words, if we want to reduce the rate of false alarms, it is probable that we will miss the exact onset of muscle activity. This fact was earlier revealed in the ROC curves (Fig. 3). Now, while comparing the performance of the two detection schemes (double threshold and energy detector), we are faced with the same dilemma. Is it desirable to have the best detection (with more false alarms), or aim to reduce number of false alarms (likely to miss exact onset of muscle activity)? In the double threshold detection scheme, once P_{FA} is fixed by the user, P_ζ, which actually serves as the false alarm probability, is calculated using Bernoulli trials. This additional process in turn reduces the user specified P_{FA}, e.g., for a P_{FA} of 0.01, P_ζ is calculated as 0.002 (standard values of parameters assumed, $m = 5, r_o = 1$). Threshold ζ is computed using this new value. Further, if any sample out of five samples of auxiliary series crosses the threshold, detection of activity is declared. Therefore, the double threshold detection scheme is

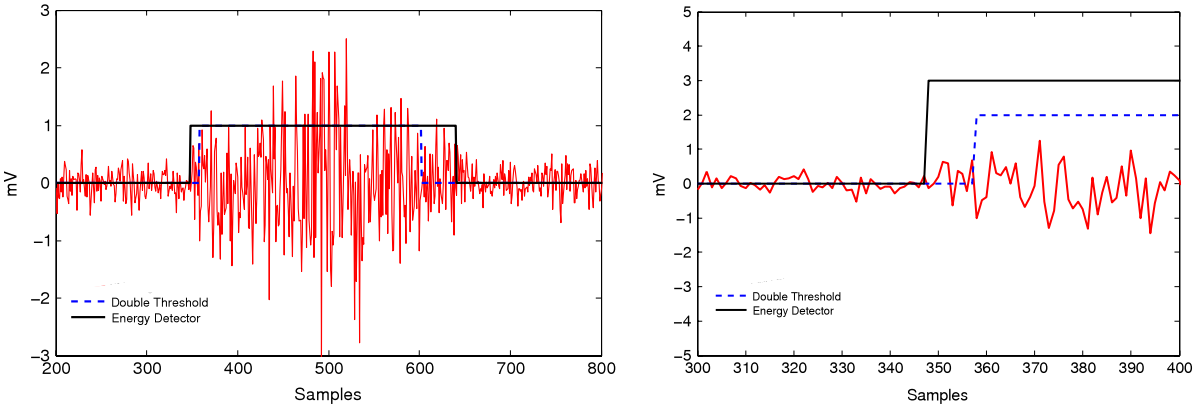

(a) Complete EMG signal. (b) Zoomed view of the same signal.

Fig. 7. Muscle activity onset detection; comparison of the detection schemes, the double threshold and the energy detector at SNR = 10.

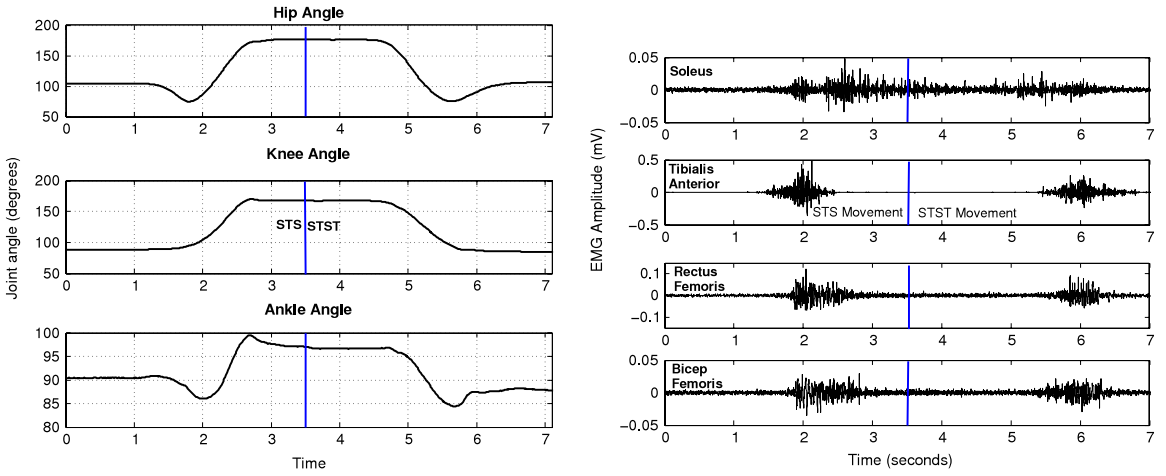

(a) Joint angles. (b) EMG signals.

Fig. 8. Kinematic profiles for three joint angles and EMG signals for one whole trial.

better at rejecting false alarms yet compromises exact onset of muscle activity detection. This compromise is depicted in Fig. 7, which clearly shows the energy detection scheme detects the onset of muscle activity more accurately than the double threshold. Despite the energy detector's more accurate identification of activation onset, for low SNR values, probability of false alarm P_{FA} is high.

6.3. *Kinematic profiles and myoelectric activity*

In addition to collecting EMG data, kinematic data based on a five point rigid link segmental model were recorded to identify temporal activations schemes. The kinematic and EMG data for a single representative trial are presented here. Fig. 8(a) shows joint angle profiles for a whole trial including both STS and STST movements with the corresponding EMG signals shown in Fig. 8(b). Regarding sequential activations timing, the tibialis anterior appears to be recruited first and has the shortest duration of recruitment, which has previously been seen [26]. The signal noise during the standing portion between movements in the other three muscles is representative of their involvement in standing postural stability. This made it difficult to identify a clear activation sequence during the STST movements. The proposed algorithms estimate variance of the noise from the samples of the EMG signals where the muscle activation (in the STS and STST transfers) has not yet clearly started. Regarding the EMG signals from the soleus, rectus femoris and bicep femoris, the noise level in the initial samples was higher, which was reflected in a higher threshold ($\acute{\gamma}$). This higher threshold observed to compromise the detection capability of the proposed detector.

In summary, if the noise levels are higher in any signal, it is difficult for the detector to make accurate decision of the muscle activity periods. As already stated, the purpose of this study is to present a comparison of the two algorithms, therefore a relatively less noisy EMG signal (recorded from muscle tibialis anterior) was selected. To determine muscle

activation periods accurately from noisy EMG data, we propose to: (a) estimate variance of the noise by first estimating noise level in the signal and then scaling the estimated noise with a parameter (λ) and (b) perform an extensive post-processing analysis based upon the selected parameter λ. Theoretically, this scheme produces promising results, which will be the focus of a future paper.

7. Conclusion

Muscle activity detection from a surface EMG signal is a challenging task due to several factors. These include inherent biological stochasticity of the EMG signal, noise added during the recording procedures, and the non-stationary nature of the EMG signal. Moreover, sequential activation of the muscle activity onset cannot be done without kinematic data. Further, some muscles may remain active after contributing to the primary movement objectives (e.g. stabilization of posture) depending upon the movement being performed. In the literature, the double threshold detection scheme has been commonly used for movements that utilize relatively large muscle forces encompassed by relative periods of inactivity. We introduced a novel detection scheme based upon energy of the signal for detecting muscle activation periods during the STS and STST transfers. The results indicated a comparable performance to the double threshold detection method. It would be beneficial to compare the energy detector to other established methods during various daily functional movement tasks to further validate its usefulness.

References

[1] S.R. Babyar, K.H. McCloskey, M. Reding, Surface electromyography of lumbar paraspinal muscles during seated passive tilting of patients with lateropulsion following stroke, Neurorehabilitation and Neural Repair 21 (2007) 127–136. PMID: 17312088.
[2] P. Cheng, C. Chen, C. Wang, W. Hong, Leg muscle activation patterns of sit-to-stand movement in stroke patients, American Journal of Physical Medicine & Rehabilitation, Association of Academic Physiatrists 83 (2004) 10–16. PMID: 14709969.
[3] R. Chen, S. Kumar, R.R. Garg, A.E. Lang, Impairment of motor cortex activation and deactivation in parkinson's disease, Clinical Neurophysiology: Official Journal of the International Federation of Clinical Neurophysiology 112 (2001) 600–607. PMID: 11275531.
[4] H. Kumru, C. Summerfield, F. Valldeoriola, J. Valls-Solé, Effects of subthalamic nucleus stimulation on characteristics of EMG activity underlying reaction time in parkinson's disease, Movement Disorders: Official Journal of the Movement Disorder Society 19 (2004) 94–100. PMID: 14743367.
[5] C. De Luca, The use of surface electromyography in biomechanics, Journal of Applied Biomechanics 13 (1997) 135–163.
[6] R.P. Di Fabio, Reliability of computerized surface electromyography for determining the onset of muscle activity, Physical Therapy 67 (1987) 43–48. PMID: 3797476.
[7] M. Lidierth, A computer based method for automated measurement of the periods of muscular activity from an EMG and its application to locomotor EMGs, Electroencephalography and Clinical Neurophysiology 64 (1986) 378–380.
[8] P.W. Hodges, B.H. Bui, A comparison of computer-based methods for the determination of onset of muscle contraction using electromyography, Electroencephalography and Clinical Neurophysiology/Electromyography and Motor Control 101 (1996) 511–519.
[9] J.H. Abbink, A. van der Bilt, H.W. van der Glas, Detection of onset and termination of muscle activity in surface electromyograms, Journal of Oral Rehabilitation 25 (1998) 365–369. PMID: 9639161.
[10] P. Bonato, T. D'Alessio, M. Knaflitz, A statistical method for the measurement of muscle activation intervals from surface myoelectric signal during gait, IEEE Transactions on Biomedical Engineering 45 (1998) 287–299.
[11] S. Micera, A.M. Sabatini, P. Dario, An algorithm for detecting the onset of muscle contraction by EMG signal processing, Medical Engineering & Physics 20 (1998) 211–215. PMID: 9690491.
[12] G. Staude, W. Wolf, Objective motor response onset detection in surface myoelectric signals, Medical Engineering & Physics 21 (1999) 449–467. PMID: 10624741.
[13] G. Staude, C. Flachenecker, M. Daumer, W. Wolf, Onset detection in surface electromyographic signals: A systematic comparison of methods, EURASIP Journal on Advances in Signal Processing 2001 (2001) 67–81.
[14] A. Merlo, D. Farina, R. Merletti, A fast and reliable technique for muscle activity detection from surface EMG signals, IEEE Transactions on Biomedical Engineering 50 (2003) 316–323.
[15] G. Vannozzi, S. Conforto, T. D'Alessio, Automatic detection of surface EMG activation timing using a wavelet transform based method, Journal of Electromyography and Kinesiology: Official Journal of the International Society of Electrophysiological Kinesiology 20 (2010) 767–772. PMID: 20303286.
[16] S. Solnik, P. DeVita, P. Rider, B. Long, T. Hortobágyi, TeagerKaiser operator improves the accuracy of EMG onset detection independent of signal-to-noise ratio, Acta of Bioengineering and Biomechanics/Wroclaw University of Technology 10 (2008) 65–68. PMID: 19032000 PMCID: 2596643.
[17] J. Bobet, R.W. Norman, Least-squares identification of the dynamic relation between the electromyogram and joint moment, Journal of Biomechanics 23 (1990) 1275–1276. PMID: 2292608.
[18] R.A. Bogey, L.A. Barnes, J. Perry, Computer algorithms to characterize individual subject EMG profiles during gait, Archives of Physical Medicine and Rehabilitation 73 (1992) 835–841. PMID: 1514893.
[19] N. Grahovac, M. Åigi, Modelling of the hamstring muscle group by use of fractional derivatives, Computers & Mathematics with Applications 59 (2010) 1695–1700.
[20] W.G.M. Janssen, H.B.J. Bussmann, H.J. Stam, Determinants of the sit-to-stand movement: a review, Physical Therapy 82 (2002) 866–879. PMID: 12201801.
[21] G.M. Ljung, G.E.P. Box, On a measure of lack of fit in time series models, Biometrika 65 (1978) 297–303.
[22] S.M. Kay, Fundamentals of Statistical Signal Processing, Volume 2: Detection Theory, first ed., Prentice Hall, 1998.
[23] N. Stergiou, Innovative Analyses of Human Movement, Human Kinetics, 2004.
[24] X. Zhao, Y. Yao, L. Yan, Learning algorithm for multimodal optimization, Computers & Mathematics with Applications 57 (2009) 2016–2021.
[25] G. Chiandussi, M. Codegone, S. Ferrero, F. Varesio, Comparison of multi-objective optimization methodologies for engineering applications, Computers & Mathematics with Applications 63 (2012) 912–942.
[26] F.R. Goulart, J. Valls-Solé, Patterned electromyographic activity in the sit-to-stand movement, Clinical Neurophysiology: Official Journal of the International Federation of Clinical Neurophysiology 110 (1999) 1634–1640. PMID: 10479031.